Materials Sciences and Applications, 2010, 1, 168-176
doi:10.4236/msa.2010.13027 Published Online August 2010 (http://www.SciRP.org/journal/msa)

Hydrogen Absorption and Electrochemical Properties of As-Quenched Nanocrystalline $Mg_{20}Ni_{10-x}Cu_x$ (x = 0 – 4) Alloys

Jinliang Gao[1], Zhonghui Hou[2], Qilu Ge[1], Dongliang Zhao[1], Shihai Guo[1], Yanghuan Zhang[1,2]

[1]Department of Functional Material Research, Central Iron and Steel Research Institute, Beijing, China; [2]School of Material, Inner Mongolia University of Science and Technology, Baotou, China.
Email: zyh59@yahoo.com.cn

Received April 20th, 2010; revised May 18th, 2010; accepted May 19th, 2010.

ABSTRACT

Nanocrystalline Mg_2Ni-type alloys with nominal compositions of $Mg_{20}Ni_{10-x}Cu_x$ (x = 0, 1, 2, 3, 4) were synthesized by rapid quenching technique. The microstructures of the as-cast and quenched alloys were characterized by XRD, SEM and HRTEM. The hydrogen absorption and desorption kinetics of the alloys were measured using an automatically controlled Sieverts apparatus. The electrochemical hydrogen storage performances were tested by an automatic galvanostatic system. The results show that all the as-quenched alloys hold a typical nanocrystalline structure, and the rapid quenching does not change the major phase Mg_2Ni. The hydrogen absorption and desorption capacities of the alloys significantly increase with rising quenching rate. Additionally, the rapid quenching significantly improves the electrochemical hydrogen storage capacity of the alloys, but it slightly impairs the cycle stability of the alloys.

Keywords: *Mg_2Ni-type Alloy, Rapid Quenching, Nanocrystalline, Hydrogen Absorption, Electrochemical Properties*

1. Introduction

Among the known alloys with a potential use in hydrogen storage, Mg and Mg-based metallic hydrides are considered to be more promising materials for hydrogen storage because of their highest hydrogen capacity and low price [1,2]. Unfortunately, some shortcomings of these kinds of metal hydrides, such as slow sorption/desorption kinetics, high dissociation temperature and poor electrochemical cycling properties, limit their practical application. Therefore, finding ways of improving the hydration kinetics of Mg-based alloys has been one of the main challenges faced by researchers in this area. Various attempts, involving mechanical alloying (MA) [3], GPa hydrogen pressure method [4], melt spinning [5], gravity casting [6], polyol reduction [7], hydriding combustion synthesis [8], surface modification [9], alloying with other elements [10,11], adding catalysts [12] etc, have been undertaken to improve the activation and hydriding properties.

Zaluska *et al.* [13] reported that a milled mixture of Mg_2NiH_4 and MgH_2 shows excellent absorption/desorption kinetics at 220-240˚C and a maximum hydrogen concentration of more than 5 wt.%. Hanada *et al.* [14] obtained a hydrogen storage capacity of 6.5 wt.% after doping MgH_2 with nanosized-Ni in a temperature range of 150-250˚C. Recham *et al.* [15] found that the hydrogen absorption property of ball-milled MgH_2 can be enhanced by adding NbF_5, and MgH_2 + 5wt.%NbF_5 composite desorbs 3 wt.% of H_2 at 150˚C. Dobrovolsky *et al.* [16] synthesized a MgH_2 (50 wt.%) + TiB_2 (50 wt.%) composite by intensive mechanical milling and found that TiB_2 addition decreases the dissociation temperature of the MgH_2 hydride by about 50˚C. The result obtained by Cui et al [17] confirmed that amorphous and/or nanocrystalline Mg-Ni-based alloys can electrochemically absorb and also desorb large amounts of hydrogen already at room temperature. Kohno *et al.* [18] obtained a large discharge capacity of 750 mAh/g at a current density of 20 mA/g for modified Mg_2Ni alloys.

Ball-milling, indubitably, is a quite powerful method for the preparation of nanocrystalline and amorphous Mg and Mg-based alloys. Particularly, it is suitable to solubilize particular elements into MgH_2 or Mg_2NiH_4 above the thermodynamic equilibrium limit. This is helpful to destabilize MgH_2 or Mg_2NiH_4 [19]. However, the milled Mg and Mg-based alloys show very poor hydrogen absorbing and desorbing stability due to the fact that the metastable

structures formed by ball milling tended to vanish during multiple hydrogen absorbing and desorbing cycles [20]. Alternatively, rapid quenching technique can overcome the above mentioned shortcoming and effective avoiding the significant degradation of hydrogen absorbing and desorbing cycle properties of Mg and Mg-based [21]. Additionally, the rapid quenching technique is an effective method to obtain a nanocrystalline structure and is very suitable for mass-production of nanocrystalline Mg-based alloys. It was also confirmed that nanocrystalline alloys produced by rapid quenching could have excellent hydriding characteristics even at room temperature, similar to the alloys produced by the MA process. Spassov *et al.* [22] prepared $Mg_2(Ni,Y)$ hydrogen storage alloy with exact composition $Mg_{63}Ni_{30}Y_7$ by rapid solidification, and its maximum hydrogen absorption capacity (about 3.0 wt.%) and hydrogenation kinetics of the as-quenched $Mg_2(Ni, Y)$ were found to exceed those of the conventionally prepared polycrystalline Mg_2Ni alloys and to be comparable to the hydrogen absorption characteristics of nanocrystalline ball-milled Mg_2Ni. Huang *et al.* [23] found that amorphous and nanocrystalline Mg- based alloy $(Mg_{60}Ni_{25})_{90}Nd_{10}$ prepared by rapid quenching obtained the highest discharge capacity of 580 mAh/g and the maximum hydrogen capacity of 4.2 wt.% H.

The objective of this work is to produce the Mg-Ni-based ternary nanocrystalline alloys by rapid quenching and to examine the hydrogen absorption and electrochemical properties of the nanocrystalline $Mg_{20}Ni_{10-x}Cu_x$ (x = 0 – 4) alloys.

2. Experimental

The nominal compositions of the experimental alloys were $Mg_{20}Ni_{10-x}Cu_x$ (x = 0, 1, 2, 3, 4). For convenience, the alloys were denoted with Cu content as Cu_0, Cu_1, Cu_2, Cu_3 and Cu_4, respectively. The alloy ingots were prepared using a vacuum induction furnace in a helium atmosphere at a pressure of 0.04 MPa. Part of the as-cast alloys was re-melted and quenched by melt-spinning with a rotating copper roller. The quenching rate was approximately expressed by the linear velocity of the copper roller because it is too difficult to measure a real quenching rate *i.e.* cooling rate of the sample during quenching. The quenching rates used in the experiment were 15, 20, 25 and 30 m/s, respectively.

The phase structures of the as-cast and quenched alloys were determined by XRD diffractometer (D/max/2400). The diffraction, with the experimental parameters of 160 mA, 40 kV and 10˚/min respectively, was performed with $CuK_{\alpha 1}$ radiation filtered by graphite. The thin film samples of the as-quenched alloys were prepared by ion etching for observing the morphology with high resolution transmission electronic microscope (HR-TEM) (JEM-2100F, operated at 200 kV), and for determining the crystalline state of the samples with electron diffraction (ED). The morphologies of the as-cast alloys were examined by scanning electronic microscope (SEM) (Philips QUANTA 400).

The hydrogen absorption and desorption kinetics of the alloys were measured by an automatically controlled Sieverts apparatus. The hydrogen absorption was conducted at 1.5MPa and the hydrogen desorption in a vacuum (1×10^{-4} MPa) at 200˚C. The alloy ribbons were pulverized and then mixed with carbonyl nickel powder in a weight ratio of 1:4. The mixture was cold pressed into round electrode pellets of 10 mm in diameter and total mass of about 1 g with a pressure of 35 MPa. A tri-electrode open cell, consisting of a metal hydride electrode, a sintered $NiOOH/Ni(OH)_2$ counter electrode and a Hg/HgO reference electrode, was used for testing the electrochemical characteristics of the experimental alloy electrodes. A 6 M KOH solution was used as electrolyte. The voltage between the negative electrode and the reference electrode was defined as the discharge voltage. In every cycle, the alloy electrode was first charged at a current density of 20 mA/g, after resting for 15 min, it was discharged at the same current density to –0.500 V cut-off voltage. The environment temperature of the measurement was kept at 30˚C.

3. Results and Discussion

3.1 Microstructure Characteristics

The XRD profiles of the as-cast and quenched Cu_2 and Cu_4 alloys are presented in **Figure 1**, showing that all the as-cast and quenched alloys display a single phase structure. The rapid quenching does not change the phase structure. Listed in **Table 1** are the lattice parameters, the cell volume and the full width at half maximum (FWHM) values of the main diffraction peaks of the as-cast and quenched Cu_2 and Cu_4 alloys which were calculated by software of Jade 6.0. It can be derived from **Table 1** that the rapid quenching causes the FWHM values of the main diffraction peaks of the alloys significantly increased and the lattice parameters and cell volume of the alloys cleverly enlarged, which is doubtless attributed to the refinement of the average grain size and stored stress in the grains produced by the rapid quenching. The crystallite size $< D_{hkl} >$ (Å) of the as-quenched alloy was calculated from the FWHM values of the broad diffraction peak (203) in **Figure 1(b)**, using Scherrer's equation. The grain sizes of the as-quenched alloys are in a range of 2-6 nm, consistent with results reported by Friedlmeier *et al.* [24]. It is important to notice that < D > values were calculated on the same peak having Miller indices (203) due to better possibility of mutual comparison.

Figure 2 shows the HRTEM micrographs and electron

diffraction pattern of the as-quenched Cu_2 and Cu_4 alloys, which display a nanocrystalline microstructure, with an average crystalline size of about 2-5 nm. From HR-TEM observations there is some evidence that the as-quenched alloys were strongly disordered and nanostructured, but they are free of amorphous phase. This result agrees very well with the XRD observation shown in **Figure 1**. The crystal defects in the as-quenched alloy, stacking faults (denoted as A), twin-grain boundaries (denoted as B), dislocations (denoted as C) and sub-grain boundaries (denoted as D) generated by rapid quenching, can clearly be seen in **Figure 3**.

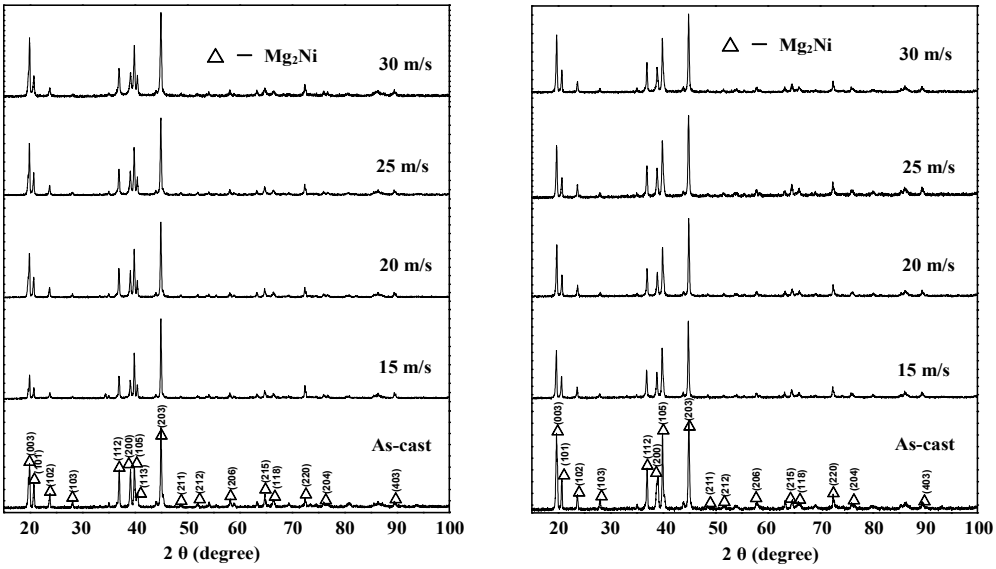

(a) (b)

Figure 1. XRD profiles of the as-cast and spun alloys: (a) Cu_2 alloy; (b) Cu_4 alloy

Table 1. The lattice parameters, cell volume and the FWHM values of the major diffraction peaks of the alloys

Quenching rates (m/s)	FWHM values				Lattice parameters and cell Volume					
	2θ(20.02˚)		2θ(45.14˚)		a (nm)		c (nm)		V (nm^3)	
	Cu_2	Cu_4	Cu_2	Cu_4	Cu_2	Cu_4	Cu_2	Cu_4	Cu_2	Cu_4
0	0.148	0.165	0.183	0.204	0.5214	0.5217	1.3283	1.3302	0.3127	0.3135
15	0.181	0.232	0.207	0.241	0.5216	0.5220	1.3293	1.3311	0.3132	0.3141
20	0.232	0.286	0.223	0.252	0.5216	0.5220	1.3307	1.3317	0.3135	0.3143
25	0.258	0.292	0.242	0.273	0.5217	0.5221	1.3311	1.3323	0.3138	0.3145
30	0.274	0.305	0.259	0.285	0.5219	0.5222	1.3316	1.3331	0.3141	0.3148

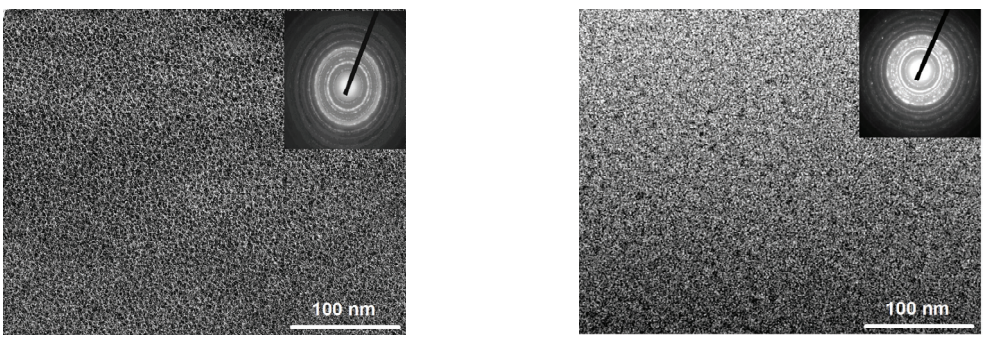

(a) (b)

Figure 2. HRTEM micrographs and ED of the as-spun alloys (30 m/s) (a) Cu_2 alloy (b) Cu_4 alloy

Shown in **Figure 4** are the SEM images of the as-cast alloy, displaying a typical dendrite structure. The substitution of Cu for Ni does not change the morphology of the alloys but it causes a significant refinement of the grains. The result obtained by energy dispersive spectrometry (EDS) indicates that the major phase of the as-cast alloys is Mg_2Ni phase (denoted as A), but Cu substitution leads to the secondary phase Mg_2Cu formed (denoted as B). This seems to be contrary with the result of XRD observation shown in **Figure 1**. It is most probably associated with the fact that Mg_2Ni and Mg_2Cu hold completely identical structure and nearly same lattice constants. On the other hand, the amount of the Mg_2Cu phase is very little so that the XRD observation can not detect the presence of the Mg_2Cu phase.

3.2 Hydriding and Dehydriding Characteristics

Figure 5 shows the hydrogen absorption capacity and kinetics of the as-cast and quenched Cu_2 and Cu_4 alloys. It can be seen that all hydriding kinetic curves of the as-quenched alloys show an initial fast hydrogen absorption stage after which the hydrogen content is saturated at longer hydrogenation time, indicating that the rapid quenching significantly improves the hydrogen absorption property of the alloys. The hydrogen absorption capacityies of the alloys increase with rising quenching rate. When the quenching rate grows from 0 (As-cast was defined as quenching rate of 0 m/s) to 30 m/s, the hydrogen absorption capacity of the Cu_2 alloy in 10 min rises from 2.33 to 3.24 wt.%, and from 1.54 to 2.72 wt.% for the Cu_4 alloy.

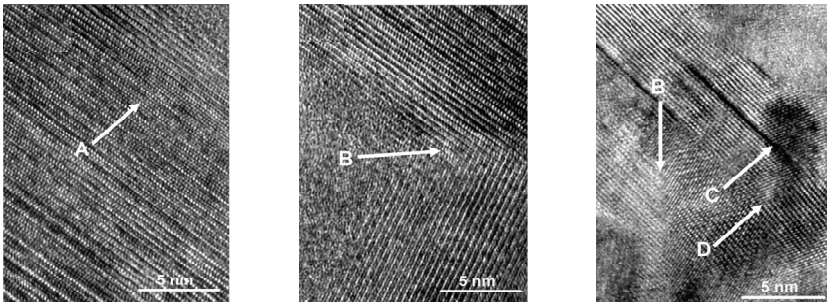

(a) (b) (c)

Figure 3. Crystal defects in the as-spun (30 m/s) Cu4 alloy taken by HRTEM

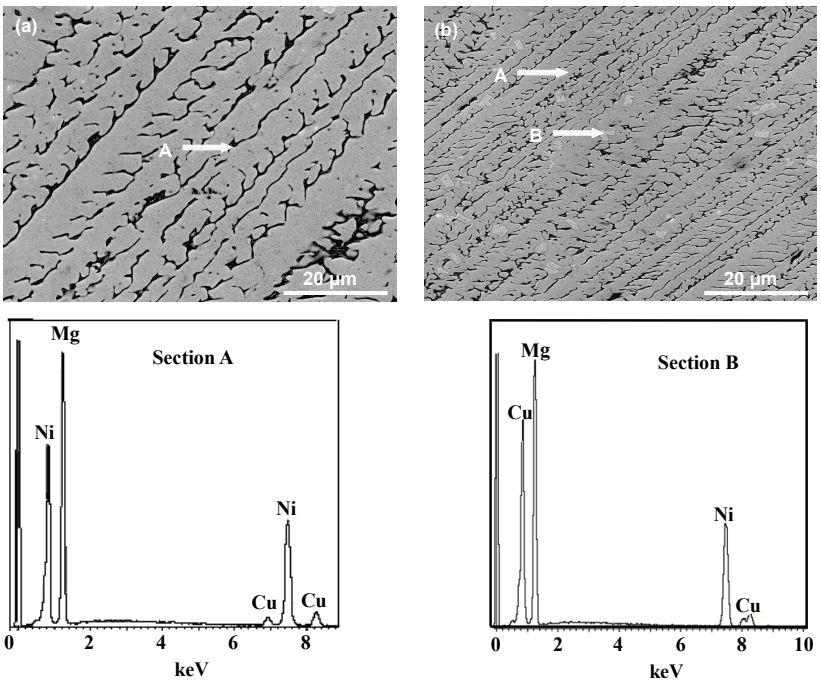

Figure 4. SEM images of the as-cast alloys with typical EDS spectra of Sections A and B in Figure 3 (b): (a) Cu_0, (b) Cu_4

The hydrogenation kinetics and storage capacity of all the as-quenched nanocrystalline Mg_2Ni-type alloys studied are superior to those of conventional polycrystalline materials with the same composition. Wu *et al.* [25] prepared Mg-10Ni-2Mm (at.%) (Mm = Ce, La-rich Mischmetal) alloy using melt spinning technology, finding that the rapid quenching treatment markedly ameliorates the kinetics of H-absorption/desorption of the alloy. A very similar result was reported by Song *et al.* [20]. The Mg-based alloys with the compositions of Mg–23.5wt% Ni and Mg–23.5wt% Ni–5wt% Cu were fabricated by rapid quenching technology. It was found that the hydriding rates of the alloys are quite high, even at 200℃. The enhanced hydrogenation property is undoubtedly associated with the refinement of the grains produced by rapid quenching [26]. By refining the microstructure, a lot of new crystallites and grain boundaries are created which can act as fast diffusion paths for hydrogen absorption. Based on the result reported by Orimo and Fujii [27], the distribution of the maximum hydrogen concentrations in three nanometer-scale regions, i.e. grain region and grain boundary region as well as amorphous region, have been experimentally determined to be 0.3 wt.% H in the grain region of Mg_2Ni, 4.0 wt.% H in the grain boundary and 2.2 wt.%H in the amorphous region. It revealed that the hydrides mainly exist in grain-bound- ary region and the amorphous phase region. The impro- ved hydrogenation characteristics can be explained with the enhanced hydrogen diffusivity in the nanocrystalline microstructure as the nanocrystalline leads to an easier access of hydrogen to the nanograins, avoiding the long- range diffusion of hydrogen through an already formed hydride, which is often the slowest stage of absorption. It is known that the nanocrystalline microstructures can accommodate higher amounts of hydrogen than polycrystalline ones. The large number of interfaces and grain boundaries available in the nanocrystalline materials provide easy pathways for hydrogen diffusion and promote the absorption of hydrogen.

Figure 6 shows the hydrogen desorption capacity and kinetics of the as-cast and quenched Cu_2 and Cu_4 alloys, indicating that the dehydriding capability of the alloys obviously meliorates with rising quenching rate. When the quenching rate increases from 0 to 30 m/s, the hydrogen

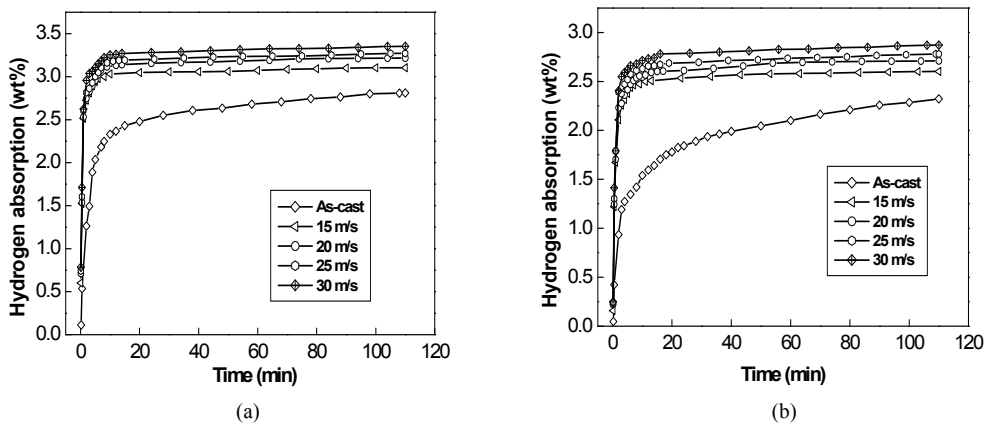

Figure 5. Hydrogen absorption kinetic curves of the as-cast and quenched alloys. (a) Cu_2 alloy; (b) Cu_4 alloy

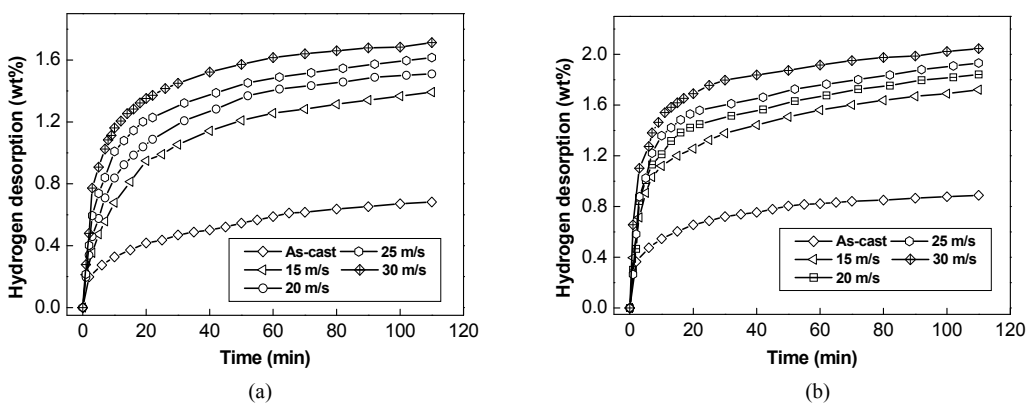

Figure 6. Hydrogen desorption kinetic curves of the as-cast and spun alloys. (a) Cu_2 alloy; (b) Cu_2 alloy

desorption capacity of the Cu_2 alloy in 20 min rises from 0.42 to 1.35 wt.%, and from 0.65 to 1.68 wt.% for Cu_4 alloy, respectively. The nanocrystalline Mg_2Ni-type alloys produced by rapid quenching exhibit higher H-absorption capacity and faster kinetics of hydriding/dehydriding than crystalline Mg_2Ni. A similar result was reported by Spassov et al [28,29]. The specific capacity and hydriding/dehydriding kinetics of hydride materials depend on their chemical composition and crystalline structure [30]. The observed essential differences in the hydriding/dehydriding kinetics of the as-quenched nanocrystalline Mg_2Ni type alloys studied most probably have to be associated with the composition of the alloys as well as with the differences in their microstructure due to the different quenching rates. It was reported that the high surface to volume ratios, *i.e.* high specific surface area, and the presence of large number of grain boundaries in nanocrystalline alloys enhance the kinetics of hydrogen absorption/desorption [28]. Zaluski *et al.* [31] and Orimo *et al.* [32] confirmed that the hydriding/dehydriding characteristics at low temperatures (lower than 200˚C) of nanocrystalline Mg_2Ni alloys prepared by mechanical alloying can be improved by reducing the grain size (20-30 nm), due to hydrogen occupation in the disordered interface phase.

3.3 Electrochemical Hydrogen Storage Characteristics

3.3.1 Activation Capability and Discharge Capacity

Electrochemical galvanostatic charge/discharge is a more effective and less time-consuming method for determining the absorbing hydrogen capacity than a gaseous technique. The influences of rapid quenching on the activation capability of the alloys were shown in **Figure 7**, and the charging-discharging current density being 20 mA/g. The figures show that all the alloys have excellent activation capabilities and attain their maximum discharge capacities at first charging-discharging cycle. The rapid quenching does not affect the activation performances of the alloys. The evolution of the maximum discharge capacities of the alloys with the quenching rate is shown in **Figure 8**. It can be derived in **Figure 8** that the discharge capacity of the alloys increases with rising quenching rate. When quenching rate increases from 0 to 30 m/s, the discharge capacity of the Cu_2 alloy enhances from 65.9 to 189.3 mAh/g, and from 53.3 to 140.4 mAh/g for Cu_4 alloy. A similar result was reported by Simičić et al [2]. It must be mentioned that the discharge capacity of the alloys containing Cu are higher than that of Cu-free alloy, suggesting that the substitution of Cu for Ni enhances the discharge capacity of the Mg_2Ni-type alloy. Two reasons are mainly responsible for this result. Firstly, the partial substitution of Cu for Ni in Mg_2Ni compound

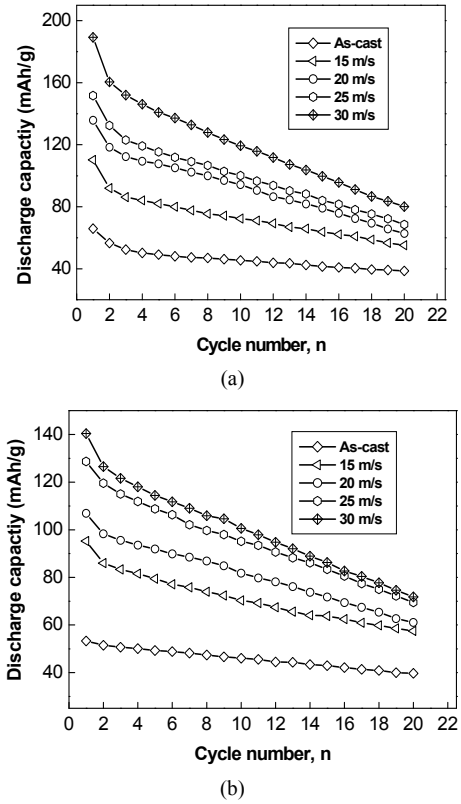

Figure 7. Evolution of the discharge capacity of the alloys with the cycle number: (a) Cu_2 alloy; (b) Cu_4 alloy

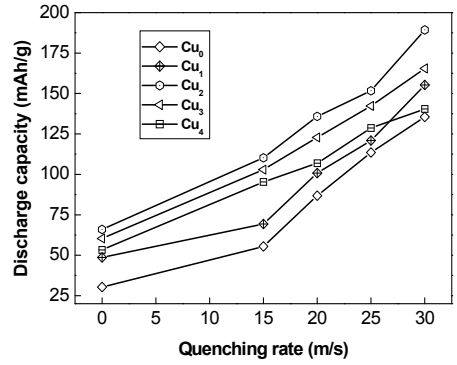

Figure 8. Evolution of the discharge capacity of the alloys with the quenching rate

may help to destabilize the hydride and activate the Mg_2Ni phase to absorb/desorb reversibly hydrogen in the alkaline electrolyte [2]. On the other hand, the secondary phase Mg_2Cu probably act as an efficient catalyst for dissociating H_2 molecules and transferring the H atoms to the surrounding Mg_2Ni matrix [20]. The observed essential differences in the discharge capacity of the alloys caused by rapid quenching most probably have to be associated with the differences in their microstructures.

The crystalline material, when rapidly quenched, becomes at least partially disordered and its structure changes to nanocrystalline. Consequently, high densities of crystal defects such as dislocations, stacking faults and grain boundaries are introduced. The densities of the crystal defects mainly depend on the quenching rate. The higher the quenching rate, the larger the densities of the crystal defects are. The large number of interfaces and grain boundaries available in the nanocrystalline materials provide easy pathways for hydrogen diffusion and accelerates the hydrogen absorbing/desorbing process. Additionally, as a result of the defects introducing distortion of crystal lattice, the stored sufficient energy as chemical disorder and the introduced defects (including both stacking faults as well as grain boundaries) will produce internal strain. It was concluded by Northwood *et al.* [33] that the exchange current density and H-diffusion coeffic ient are directly proportional to the internal strain. Therefore, it is understandable that the introduction of defects, disordering and internal strain leads to an increasing hydriding/dehydriding rates and capacity.

3.3.2 Charging and Discharging Cycle Stability

The cycle stability of the electrode alloy is a decisive factor of the life of the Ni-MH battery. The capacity retaining rate (S_n), which was introduced to evaluate accurately the cycle stability of the alloy, is defined as $S_n = C_n/C_{max} \times 100\%$, where C_{max} is the maximum discharge capacity and C_n is the discharge capacity of the nth charge-discharge cycle, respectively. According to the above menti- oned definition, it can be known that the larger the cap- acity retaining rate (S_n), the better the cycle stability of the alloy. The evolution of the capacity retaining rate (S_{20}) of the alloys with quenching rate is illustrated in **Figure 9**. The figure show that the capacity retaining rate (S_{20}) of the alloys clearly declines with rising quenching rate. When quenching rate increases from 0 to 30 m/s, the capacity retaining rate of the Cu_2 alloy after 20 cycles falls from 58.6 to 42.3%, and from 74.4 to 51.1% for the Cu_4 alloy. It can also be seen in **Figure 9** that, for a fixed quenching rate, the capacity retaining rate of the alloys mounts up with rising Cu content, reflecting that the substitution of Cu for Ni enhances the cycle stability of the alloys. In order to clearly see the process of the capacity degradation of the alloy electrode, the evolution of the capacity retaining rate of the as-cast and quenched Cu_2 and Cu_4 alloys with the cycle number is shown in **Figure 10**. A rough tendency can be seen in the **Figure 10** that the rapid quenching causes an increase of the decay rates of the discharge capacities of the alloys, suggesting that the rapid quenching impairs the cycle stability of the alloys. It was well known that the essential reason of which leads to the capacity degradation of the Mg-based alloy electrodes is the severe corrosion of Mg in the alkaline KOH solution. Especially, during the discharging process, the alloys are anodically polarized so that corrosion would be faster [2]. On the other hand, the metastable structures formed by rapid quenching or ball milling tended to vanish during multiple charging/discharging cycles, which is an important factor for the capacity decay of the alloys. Two reasons are responsible for the enhanced cycle stability of the Mg_2Ni-type alloy by Cu substitution.

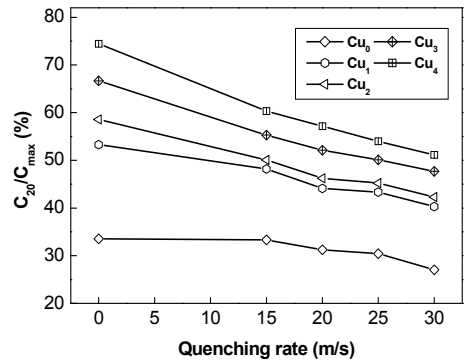

Figure 9. Evolution of the capacity retaining rate (S_{20}) of the alloys with the quenching rate

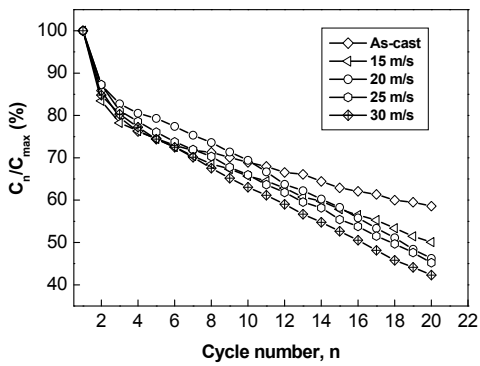

(a)

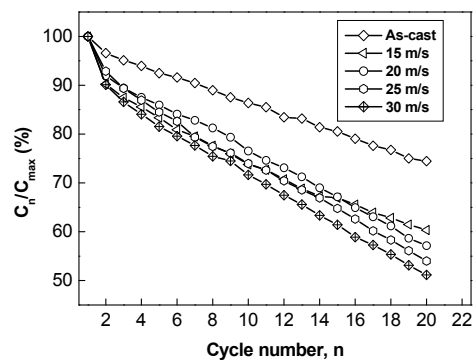

(b)

Figure 10. Evolution of the capacity retaining rate of the as-cast and quenched alloys with cycle number (a) Cu_2 alloy; (b) Cu_4 alloy

Firstly, the improved performance in the cycle life of substituted alloy electrodes is presumably attributed to preferential oxidation of Cu on the alloy surface and the prevention of the formation of the $Mg(OH)_2$ passive layer. Secondly, the additive of a third element significantly stabilizes the nanostructure of Mg-Ni-based alloy [28], reflecting an increase of the cycle stability of the alloy. The nanostructure of the alloys formed by rapid quenching was detrimental for corrosion in the electrolyte during cycling due to the fact that intercrystalline corrosion is inevitable. Therefore, it is comprehensible why rapid quenching leads to a decline of the cycle stability of the Mg-Ni-Cu system alloy.

4. Conclusions

The structures and hydrogen storage characteristics of the nanocrystalline $Mg_{20}Ni_{10-x}Cu_x$ (x = 0 – 4) alloys were investigated, and the conclusions obtained are summarized as follows:

1) All the as-quenched $Mg_{20}Ni_{10-x}Cu_x$ (x = 0 – 4) alloys hold nanocrystalline structures and are free of amorphous phase. The rapid quenching does not change the major phase of Mg_2Ni-type in the alloy, but it leads to an increment of the lattice parameters and cell volume as well as the FWHM values of the major diffraction peaks of the alloys.

2) Rapid quenching significantly improves the hydriding and dehydriding properties of the alloys. Hydriding and dehydriding capacities and rates of the alloy markedly rise with increasing quenching rate.

3) Additionally, rapid quenching considerably enhances the electrochemical discharge capacity of the alloys, whereas it slightly weakens the charging/discharging cycle stability of the alloys, for which the nanocrystalline structure formed by rapid quenching is basically responsible.

5. Acknowledgements

This work is supported by Hi-Tech Research and Development Program of China (2007AA03Z227), National Natural Science Foundations of China (50871050 and 50701011), Natural Science Foundation of Inner Mongolia, China (200711020703) and Higher Education Science Research Project of Inner Mongolia, China (NJzy 08071).

REFERENCES

[1] L. Schlapbach and A. Züttel, "Hydrogen-Storage Materials for Mobile Applications," *Journal of Nature*, Vol. 414, 2001, pp. 353-358.

[2] M. V. Simičić, M. Zdujić, R. Dimitrijević, L. Nikolić-Bujanović and N. H. Popović, "Hydrogen Absorption and Electrochemical Properties of Mg_2Ni-Type Alloys Synthesized by Mechanical Alloying," *Journal of Power Sources*, Vol. 158, No. 1, 2006, pp. 730-734.

[3] A. Ebrahimi-Purkani and S. F. Kashani-Bozorg, "Nanocrystalline Mg_2Ni-Based Powders Produced by High-Energy Ball Milling and Subsequent Annealing," *Journal of Alloys and Compounds*, Vol. 456, No. 1-2, 2008, pp. 211-215.

[4] D. Kyoi, T. Sakai, N. Kitamura, A. Ueda and S. Tanase, "Synthesis of FCC Mg-Ta Hydrides Using GPa Hydrogen Pressure Method and their Hydrogen-Desorption Properties," *Journal of Alloys and Compounds*, Vol. 463, No. 1-2, 2008, pp. 306-310.

[5] P. Palade, S. Sartori, A. Maddalena, G. Principi, S. Lorusso, M. Lazarescu, G. Schinteie, V. Kuncser and G. Filoti, "Hydrogen Storage in Mg-Ni-Fe Compounds Prepared by Melt Spinning and Ball Milling," *Journal of Alloys and Compounds*, Vol. 415, No. 1-2, 2006, pp. 170-176.

[6] M. Y. Song, C. D. Yim, J. S. Bae, D. R. Mummd and S. H. Hong, "Preparation by Gravity Casting and Hydrogen-Storage Properties of Mg—23.5 wt.% Ni—(5, 10 and 15 wt.%) La," *Journal of Alloys and Compounds*, Vol. 463, No. 1-2, 2008, pp. 143-147.

[7] L. H. Kumar, B. Viswanathan and S. S. Murthy, "Hydrogen Absorption by Mg_2Ni Prepared by polyol Reduction," *Journal of Alloys and Compounds*, Vol. 461, No. 1-2, 2008, pp. 72-76.

[8] X. F. Liu, Y. F. Zhu and L. Q. Li, "Structure and Hydrogenation Properties of Nanocrystalline Mg_2Ni Prepared by Hydriding Combustion Synthesis and Mechanical Milling," *Journal of Alloys and Compounds*, Vol. 455, No. 1-2, 2008, pp. 197-202.

[9] F. J. Liu and S. Suda, "A Method for Improving the Long-Term Storability of Hydriding Alloys by Air Water Exposure," *Journal of Alloys Compounds*, Vol. 231, No. 1-2, 1995, pp. 742-750.

[10] T. Czujko, R. A. Varin, C. Chiu and Z. Wronski, "Investigation of the Hydrogen Desorption Properties of Mg + 10 wt.% X (X = V, Y, Zr) Submicrocrystalline Composites," *Journal of Alloys Compounds*, Vol. 414, No. 1-2, 2006, pp. 240- 247.

[11] C. X. Shang, M. Bououdina, Y. Song and Z. X. Guo, "Mechanical Alloying and Electronic Simulations of (MgH_2 + M) Systems (M = Al, Ti, Fe, Ni, Cu and Nb) for Hydrogen Storage," *International Journal of Hydrogen Energy*, Vol. 29, No. 1, 2004, pp. 73-80.

[12] B. Sakintuna, F. Lamari-Darkrim and M. Hirscher, "Metal Hydride Materials for Solid Hydrogen Storage: A Review," *International Journal of Hydrogen Energy*, Vol. 32, No. 9, 2007, pp. 1121-1140.

[13] A. Zaluska, L. Zaluski and J. O. Stroem-Olsen, "Synergy of Hydrogen Sorption in Ball-Milled Hydrides of Mg and Mg_2Ni," *Journal of Alloys Compounds*, Vol. 289, No. 1-2, 1999, pp. 197-206.

[14] N. Hanada, T. Ichikawa and H. Fujii, "Catalytic Effect of Nanoparticle 3d-Transition Metals on Hydrogen Storage

Properties in Magnesium Hydride MgH_2 Prepared by Mechanical Milling," *Journal of Physical Chemistry B*, Vol. 109, No. 15, 2005, pp. 7188-7194.

[15] N. Recham, V. V. Bhat, M. Kandavel, L. Aymard, J. M. Tarascon and A. Rougier, "Reduction of Hydrogen Desorption Temperature of Ball-Milled MgH_2 by NbF_5 Addition," *Journal of Alloys Compounds*, Vol. 464, No. 1-2, 2008, pp. 377-382.

[16] V. D. Dobrovolsky, O. G. Ershova, Y. M. Solonin, O. Y. Khyzhuna and V. Paul-Boncour, "Influence of TiB_2 Addition upon Thermal Stability and Decomposition Temperature of The Mgh_2 Hydride of a Mg-Based Mechanical Alloy," *Journal of Alloys Compounds*, Vol. 465, No. 1-2, 2008, pp. 177-182.

[17] N. Cui, B. Luan, H. J. Zhao, H. K. Liu and S. X. Dou, "Effects of Yttrium Additions on the Electrode Performance of Magnesium-Based Hydrogen Storage Alloys," *Journal of Alloys Compounds*, Vol. 233, No. 1-2, 1996, pp. 236- 240.

[18] T. Kohno and M. Kanda, "Effect of Partial Substitition on Hydrogen Storage Properties of Mg2Ni Alloy," *Journal of Electrochemical Society*, Vol. 144, 1997, pp. 2384-2388.

[19] G. Y. Liang, "Synthesis and Hydrogen Storage Properties of Mg-Based Alloys," *Journal of Alloys Compound*s, Vol. 370, No. 1-2, 2004, pp. 123-128.

[20] M. Y. Song, S. N. Kwon, J. S. Bae and S. H. Hong, "Hydrogen-Storage Properties of Mg–23.5Ni–(0 and 5)Cu Prepared by Melt Spinning and Crystallization Heat Treatment," *International Journal of Hydrogen Energy*, Vol. 33, No. 6, 2008, pp. 1711-1718.

[21] M. Savyak, S. Hirnyj, H. D. Bauer, M. Uhlemann, J. Eckert, L. Schultz and A. Gebert, "Electrochemical Hydrogenation of $Mg_{65}Cu_{25}Y_{10}$ Metallic Glass," *Journal of Alloys Compounds*, Vol. 364, No. 1-2, 2004, pp. 229-237.

[22] T. Spassov and U. Köster, "Electrode Properties of Melt-Spun Mg–Ni–Nd Amorphous Alloys," *Journal of Power Sources*, Vol. 160, No. 1, 2006, pp. 684-687.

[23] G. Friedlmeier, M. Arakawa, T. Hiraia and E. Akiba, "Preparation and Structural, Thermal and Hydriding Characteristics of Melt-Spun Mg–Ni Alloys," *Journal of Alloys Compounds*, Vol. 292, No. 1-2, 1999, pp. 107-117.

[24] Y. Wu, W. Han, S. X. Zhou, M. V. Lototsky, J. K. Solberg and V. A. Yartys, "Microstructure and Hydrogenation Behavior of Ball-Milled and Melt-Spun Mg–10Ni–2Mm Alloys," *Journal of Alloys and Compounds*, Vol. 466, No. 1-2, 2008, pp. 176-181.

[25] K. Tanaka, Y. Kanda, M. Furuhashi, K. Saito, K. Kuroda, H. Saka, "Improvement of Hydrogen Storage Properties of Melt-Spun Mg–Ni–RE Alloys by Nancrystallization," *Journal of Alloys Compounds*, Vol. 295, 1999, pp. 521-525.

[26] S. Orimo and H. Fujii, "Materials Science of Mg-Ni-Based New Hydrides" *Journal Applied Physics A*, Vol. 72, No. 2, 2001, pp. 167-186.

[27] T. Spassov and U. Köster, "Thermal Stability and Hydriding Properties of Nanocrystalline Melt-Spun $Mg_{63}Ni_{30}Y_7$ Alloy," *Journal of Alloys Compounds*, Vol. 279, 1998, pp. 279-286.

[28] T. Spassov, L. Lyubenova, U. Köster and M. D. Baró, "Mg–Ni–RE Nanocrystalline Alloys for Hydrogen Storage," *Journal of Materials Science and Engineering A*, Vol. 375-377, 2004, pp. 794-799.

[29] G. Mulas, L. Schiffini and G. Cocco, "Mechanochemical Study of the Hydriding Properties of Nanostructured Mg_2Ni–Ni Composites," *Journal of Materials Research*, Vol. 19, 2004, pp. 3279-3289.

[30] L. Zaluski, A. Zaluska and J. O. Ström-Olsen, "Nanocrystalline Metal Hydrides," *Journal of Alloys Compounds*, Vol. 2532, No. 54, 1997, pp. 70-79.

[31] S. Orimo, H. Fujii and K. Ikeda, "Notable Hydriding Properties of a Nanostructured Composite Material of the Mg_2Ni-H System Synthesized by Reactive Mechanical Grinding," *Acta Materialia*, Vol. 45, No. 1, 1997, pp. 331-341.

[32] H. Niu and D. O. Northwood, "Enhanced Electrochemical Properties of Ball-Milled Mg_2Ni Electrodes," *International Journal of Hydrogen Energy*, Vol. 27, No. 1, 2002, pp. 69-77.

